JACS
JOURNAL OF THE AMERICAN CHEMICAL SOCIETY
pubs.acs.org/JACS
Article

Reticular Ratchets for Directing Electrochemiluminescence

Rengan Luo,[#] Xiao Luo,[#] Haocheng Xu, Sushu Wan, Haifeng Lv, Beier Zou, Yufei Wang, Tianrui Liu, Chuang Wu, Qizhou Chen, Siqi Yu, Pengfei Dong, Yuxi Tian, Kai Xi, Shuai Yuan,* Xiaojun Wu,* Huangxian Ju, and Jianping Lei*

Cite This: *J. Am. Chem. Soc.* 2024, 146, 16681−16688

Read Online

ACCESS | Metrics & More | Article Recommendations | Supporting Information

ABSTRACT: Electrochemiluminescence (ECL) involves charge transfer between electrochemical redox intermediates to produce an excited state for light emission. Ensuring precise control of charge transfer is essential for decoding ECL fundamentals, yet guidelines on how to achieve this for conventional emitters remain unexplored. Molecular ratchets offer a potential solution, as they enable the directional transfer of energy or chemicals while impeding the reverse movement. Herein, we designed 10 pairs of imine-based covalent organic frameworks as reticular ratchets to delicately manipulate the intrareticular charge transfer for directing ECL transduction from electric and chemical energies. Aligning the donor and acceptor (D−A) directions with the imine dipole effectively facilitates charge migration, whereas reversing the D−A direction impedes it. Notably, the ratchet effect of charge transfer directionality intensified with increasing D−A contrast, resulting in a remarkable 680-fold improvement in the ECL efficiency. Furthermore, dipole-controlled exciton binding energy, electron/hole decay kinetics, and femtosecond transient absorption spectra identified the electron transfer tendency from the N-end toward the C-end of reticular ratchets during ECL transduction. An exponential correlation between the ECL efficiency and the dipole difference was discovered. Our work provides a general approach to manipulate charge transfer and design next-generation electrochemical devices.

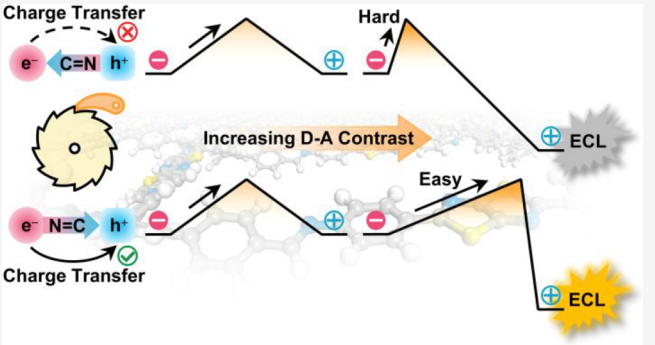

INTRODUCTION

The molecular ratchet allows the directional transfer of energy or chemicals while impeding the reverse movement,[1] finding applications in a broad range of chemical and biochemical processes.[2−4] In biological systems, directional movement can be accomplished through protein motors such as the kinesin, myosin, and dynein superfamilies.[5] Artificial molecular machines involving catenanes and rotaxanes can achieve directional movement under various stimuli, such as light, electrochemical gradient, pH, heat, solvent polarity, and cation or anion binding.[6] Benefiting from the tunable crystalline structure of metal−organic frameworks (MOFs) and covalent organic frameworks (COFs),[7−11] integrating molecular ratchet into reticular materials allows for the design of molecular ratchet with atomic precision. Moreover, periodically arranging molecular ratchets into extended network structures amplifies the ratchet effect, yielding unprecedented properties.[12,13] For example, Stoddart and co-workers developed MOF-based pumping cassettes with molecular ratchet structures for adsorption control and chemical energy storage.[14] Furthermore, reticular materials utilizing molecular ratchets to control charge transfer directions within reticular structures hold promise in diverse areas, including organic (opto)electronics, electrochemistry, photocatalysis,[15] and electrochemiluminescence (ECL).

ECL is a light-emitting process from transductions of chemical and electric energies, where excited states depend critically on the charge transfer between the electrochemically generated radical anions and cations.[16−18] For conventional emitters, ECL is generated through random collisions between radical anions and cations, leading to a low ECL efficiency. In reticular emitters, the ECL efficiency is determined by intrareticular charge transfer (IRCT)-mediated radical annihilation.[19−21] Therefore, it is intriguing to convert unbiased charge transport into directional motion by the ratchet effect to promote exciton generation for ECL emission.[19,22] Moreover, benefiting from the low background of ECL,[23−25] the ratchet effect-directed charge migration behaviors could be projected by ECL performances. However, no reticular ratchets have

Received: March 20, 2024
Revised: May 24, 2024
Accepted: May 24, 2024
Published: June 5, 2024

https://doi.org/10.1021/jacs.4c03981
J. Am. Chem. Soc. 2024, 146, 16681−16688

been designed for this purpose to our knowledge, and there is a need for suitable techniques and theories to quantify the ratchet efficiency in directing IRCT.

In this study, we designed a series of imine COFs as reticular ratchets to manipulate the IRCT for directing ECL transduction. These COF ratchets, with varying donor−acceptor (D−A) contrasts, allowed us to transduce nonequilibrium electron−hole coexistence states established through the electrochemical reaction under different ratchet potentials. Notably, we observed that the ratchet effect intensified with increasing D−A contrast, resulting in a remarkable 680-fold enhancement in the ECL efficiency. Investigations into the electronic structures of these COFs and corresponding model compounds (MCs) revealed that CH═N dipoles within the frameworks acted as ratchet teeth. Aligning the CH═N dipoles along the D−A direction effectively facilitated charge migration for ECL exciton production, whereas reversing the D−A direction significantly impeded charge transfer. This ratchet effect is supported by the delocalized band distributions, overlapped ground and excited states, and increased exciton binding energies during electron−hole recombination. Furthermore, nonadiabatic molecular dynamics (NAMD) simulation and femtosecond transient absorption (fs-TA) spectra elucidated the charge recombination dynamics, confirming the transduction efficacy of this ratchet. Overall, our study demonstrates the effective application of the ratchet effect in directing the IRCT within COFs, offering inspiration for further advancements in manipulating charge migration in reticular materials.

RESULTS AND DISCUSSION

Construction of Reticular Ratchets. Considering that ECL is generated through the annihilation of electrons and holes, a nonequilibrium state could be established via electrochemical excitation (Figures 1a and S1).[16,26] Furthermore, a series of D−A building units were selected to create nonequilibrium states with different ratchet potentials. Benefiting from the tunability of COFs, we delicately designed 10 pairs of COF-based ratchets with mutually reversed orientations of polar CH═N bonds between D−A units. We anticipated that the polarized CH═N bonds could serve as ratchet teeth, which preferentially direct the electron transfer from the N-end units to the C-end units and impede the reversed electron migration during electron−hole combination (Figure 1a), in analogy to the recently reported "ICT Tesla Valve."[15,27−29] Similar to the space charge in semiconductor heterojunctions, the CH═N bond in COFs with reversed orientation could cause inverted band bending (Figures 1b and S2), where the C-end band bends upward, and the N-end band bends downward.[30−33] Consequently, the direction of CH═N bonds not only affects the conduction band minimum (CBM) and valence band maximum (VBM) but also dictates the electron−hole combination and the resulting ECL performance (Figure 1c).

In addition to imine bonds, the electronic structures and ECL properties of COFs could be manipulated by the choice of the D−A building units. We selected 10 D−A pairs as building units and checked their electron/hole affinities through electrostatic potentials and frontier orbital analysis (Figures S3 and S4).[34] The electron-donating abilities of the building units follow the order triphenylamine (Tpa), tetraphenylpyrene (Tpy), tetraphenylethylene (Tpe), benzene (Ph), diphenylbenzothiadiazole (Bt), diphenylthiazolothiazole

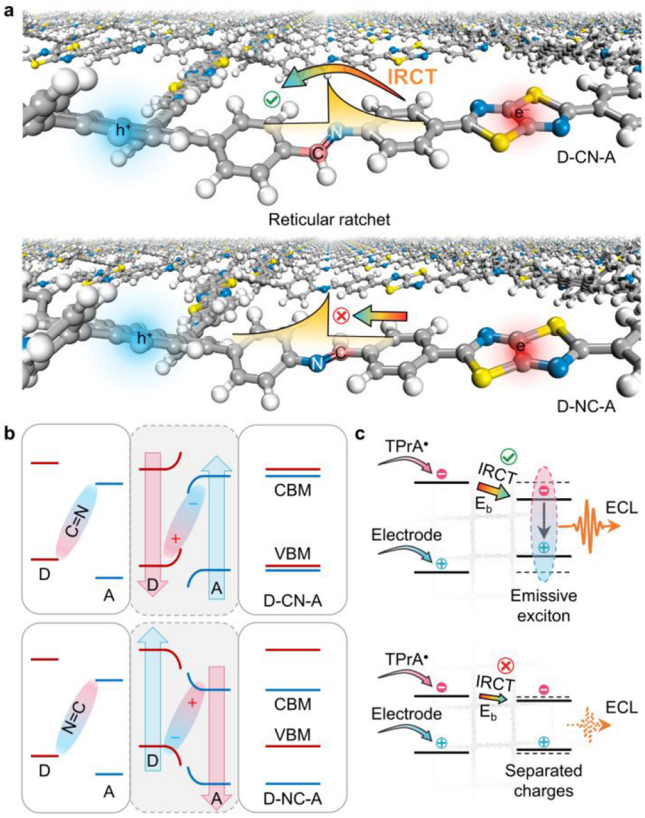

Figure 1. (a) Schematic illustration of the charge transfer direction during electron−hole recombination in the COF structures and the corresponding ratchet effect. The opposite orientations of imine bonds invert the ratchet teeth. (b) Diagrams of imine bond orientation-induced band shift. The VBM and CBM levels of D−A COFs are dominated by the electronic interactions between imine bonds and D−A units. (c) Ratchet effect-directed ECL generation. The D-CN-A with large E_b directs IRCT between the electrochemically produced electrons and holes and facilitates ECL generation, distinguishing weak ECL of D-NC-A.

(Tt), and triphenyltriazine (Tz). To further evaluate the contrasts between D−A pairs, we calculated charges and imine dipoles for 20 model compounds (Figures S5 and S8 and Table S2). The imine dipole differences align with the differential charge differences among the D−A units within each pair of models, arising from distinct electronic interactions with CH═N bonds in different orientations. The positive proportions, as shown in Figure S7, indicate that larger imine dipole differences correspond to larger D−A contrasts; thus, the latter could be quantified by the imine dipole differences. In the model pairs with large D−A contrasts, D-NC-A generally exhibits an elevated highest occupied molecular orbital (HOMO) and a reduced lowest unoccupied molecular orbital (LUMO) compared to D-CN-A (with reversed CH═N bond orientation), leading to the smaller band gaps of D-NC-A (Figure S9).

Next, we successfully synthesized 10 pairs of COF-based reticular ratchets, each featuring distinct D−A pairs and reversed CH═N bond orientations (Figure 2a and Table S1). Through optimization of solvents and acetic concentrations, each COF pair exhibits similar powder X-ray diffraction (PXRD) patterns and closely matched lattice parameters, as confirmed by the Pawley refinements (Figures S10−S20). Taking the Tpy-Tt pair (Tpy-CN-Tt and Tpy-NC-Tt COF) as

https://doi.org/10.1021/jacs.4c03981
J. Am. Chem. Soc. 2024, 146, 16681−16688

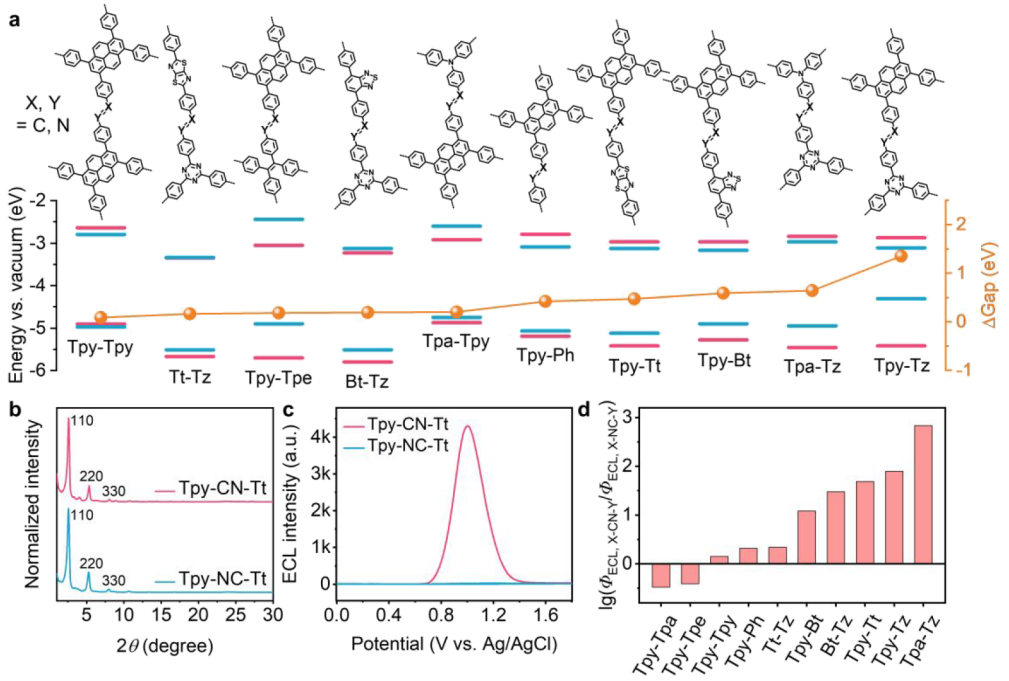

Figure 2. (a) Chemical structures and energy levels of VBM and CBM of 10 COF pairs with different D−A contrasts and corresponding band gap differences. COF pairs were designed by aligning the imine dipole along (X═C, Y═N) or against (X═N, Y═C) the D−A directions. (b) PXRD and (c) corresponding ECL patterns of the Tpy-CN-Tt and Tpy-NC-Tt pair. (d) ECL efficiency ratios of C═N to N═C linked COFs. X and Y represent the left and right ligands, respectively.

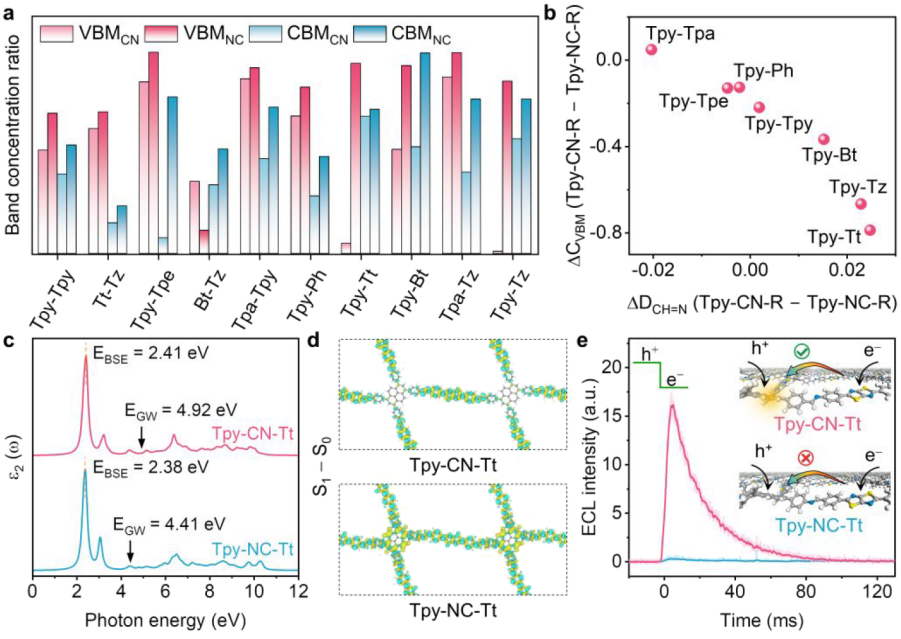

Figure 3. (a) Concentration ratio of VBM on the donor and CBM on the acceptor of reticular ratchets in spatial distribution. (b) Dependence of concentration ratio differences of VBM on dipole differences for Tpy-CN-R and Tpy-NC-R pairs. R = Tpa, Tpe, Tpy, Bt, Tt, Tz, and Ph. (c) BSE spectra of Tpy-Tt pairs. (d) Differential charge density between the 1st excited state and the ground state of the Tpy-Tt pair. Electron gain and loss are denoted as cyan and yellow, respectively. (e) ECL transients of Tpy-Tt ratchet under stepping potentials from +1.0 to −2.1 V.

an example (Figure 2b), they both show characteristic peaks at 2.68°, 5.37°, and 8.10°, corresponding to the (110), (220), and (330) crystallographic planes, respectively. This is consistent with the high-resolution transmission electron microscopy experiments, which reveal similar lattice spacings for each COF pair (Figures S21−S30). N_2 adsorption isotherms further confirm their comparable pore sizes and Brunauer−Emmett−Teller surface areas (Figures S31 and S32 and Table S3).

Despite their analogous framework structures, Fourier transform infrared spectra of D-CN-A exhibit blue-shifted stretching vibration peaks of imine bonds compared to their D-NC-A counterparts, indicating the presence of stronger dipoles in D-CN-A (Figure S33).[35] Additionally, the ^{13}C cross-

https://doi.org/10.1021/jacs.4c03981
J. Am. Chem. Soc. 2024, 146, 16681−16688

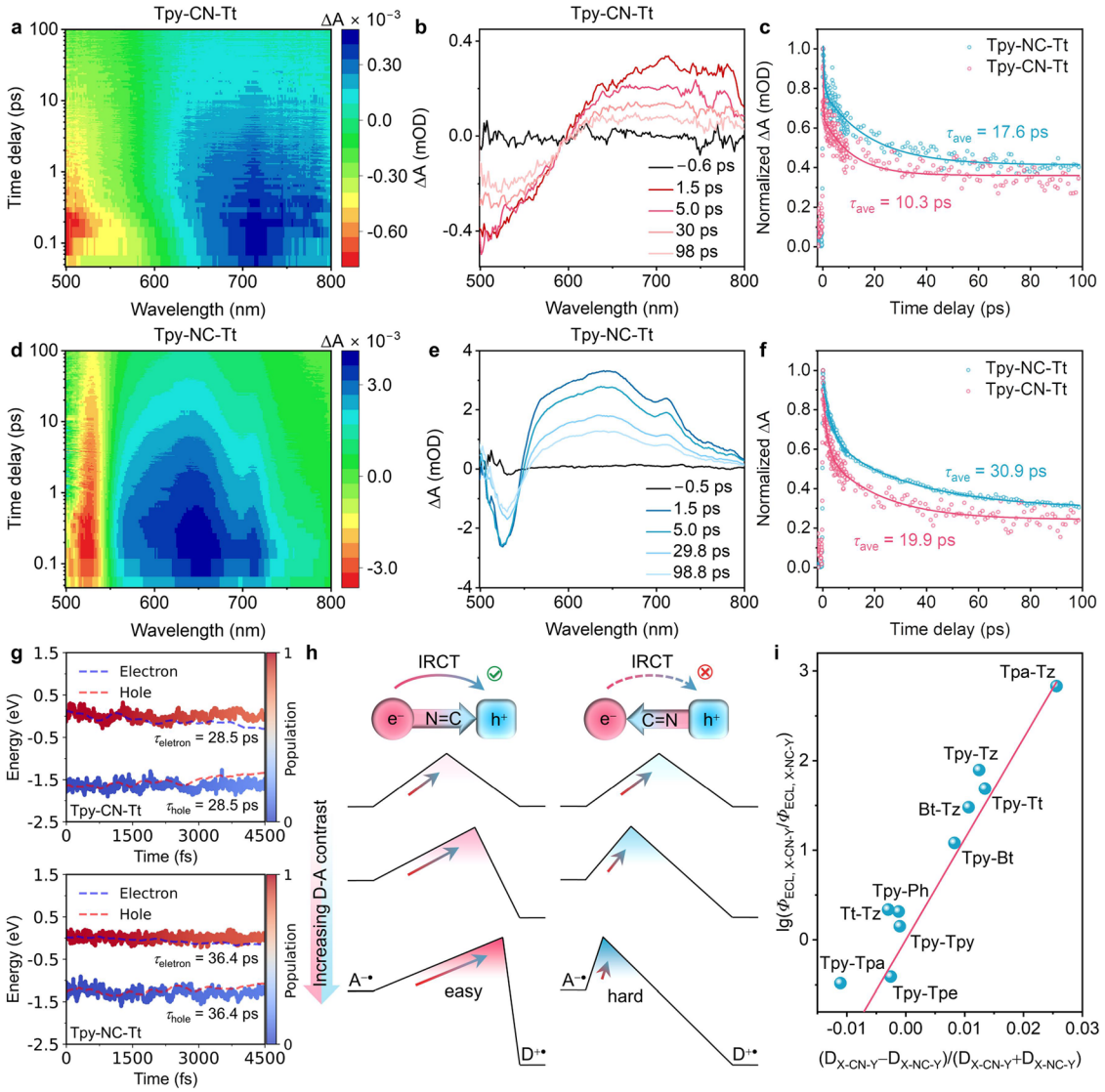

Figure 4. TA spectra of (a) Tpy-CN-Tt and (d) Tpy-NC-Tt under 420 nm excitation and (b,e) corresponding spectral cross sections at different delay times. (c) GSB and (f) ESA TA kinetics at 509 and 712 nm for Tpy-CN-Tt, and 525 and 643 nm for Tpy-NC-Tt, respectively. (g) NAMD simulations of electron and hole decay kinetics of Tpy-Tt ratchet. (h) Schematic mechanism of the D−A contrast-dependent ratchet effect in directing electron−hole recombination. In D-CN-A COFs, raising the D−A contrasts could reduce the slope of the ratchet potential and facilitate electron−hole recombination. Conversely, the slope increase of the ratchet potentials impedes charge transfer in D-NC-A COFs. (i) Correlation between ECL efficiency ratios and imine bond dipoles of reticular ratchets.

polarization magic-angle-spinning solid-state NMR experiment (Figure S34) demonstrates a downfield shift of resonances for CH═N in D-CN-A, indicative of a more electron-deficient carbon environment,[36] which is consistent with the calculated charge of imine bonds in these COFs (Figure S5c).

Furthermore, in COF pairs with substantial D−A contrasts (such as Tpy-Bt, Tpy-Tt, and Tpa-Tz), reversing the imine bonds from D-CN-A to D-NC-A caused a significant increase in VBMs and a decrease in CBMs based on density functional theory (DFT) computations (Figure 2a). Consequently, larger band gaps were obtained for D-CN-A compared to D-NC-A (Figures S35−S37). This trend is consistent with the experimentally observed redshift of fluorescence peaks and absorbance peaks in the photoluminescence and solid-state UV−vis spectra, respectively (Figures S35 and S38). Conversely, for reticular ratchets with relatively small D−A contrasts (such as Tpy-Tpy and Tt-Tz), reversing the imine bond orientation resulted in negligible differences in band gaps, fluorescence, and UV−vis absorbance peak shifts. The results are in good consistence with the proposed imine bond orientation-induced band shift model (Figures 1b and S2), verified by the experimental energy levels of Tt-Tz and Tpy-Tt COFs calculated from the ultraviolet photoelectron spectrum and Tauc plots (Figures S36, S37, and S39).

Ratcheting IRCT in ECL. The imine bond orientations could have a significant impact on IRCT-mediated electron and hole annihilation during ECL generation. As shown in Figure 2c, Tpy-CN-Tt showed a 165-fold enhancement in ECL intensity compared to that of Tpy-NC-Tt. This trend remains consistent when employing various solvents and coreactants (Figures S40−S42). We collected the ECL curves of 10 COF pairs (Figures S43 and S52), and the ratios of ECL efficiencies are presented in Figure 2d. Among them, the Tpa-Tz COF pair (characterized by the largest D−A contrast) showcases the highest ECL efficiency ratio of 680-fold by switching imine bond directions, whereas the Tpy-Tpy COF pair (featuring the

https://doi.org/10.1021/jacs.4c03981
J. Am. Chem. Soc. 2024, 146, 16681−16688

smallest D−A contrast) displays the lowest ECL efficiency ratio of 1.20-fold.

To comprehend the factors contributing to the variation in ECL upon reversing the imine bond orientations, we conducted band structure calculations for these COF pairs (Figures S53−S62). In Tpy-CN-Tt, the VBM and CBM exhibit delocalization over both the Tt and Tpy units. Conversely, in Tpy-NC-Tt, the VBM localizes at Tpy units, while the CBM localizes at Tt units (Figure S56). We introduced a concept called "band concentration ratio" to quantify the degree of charge localization for the CBM and VBM (see Supporting Information, Figure 3a and Table S4). Notably, an inverse proportion was observed between the concentration ratio differences of VBM and the dipole differences arising from the imine bond orientation in Tpy-based reticular ratchets (Figure 3b). This result implies that reversing the CH═N bond orientation in Tpy-CN-R leads to increased band localization, while a larger D−A contrast further promotes the degree of band localization. A similar trend was also observed in Tz-based COF pairs (Figure S63).

As the ECL is related to exciton generation (Figures S63 and S64),[16,22,37] we proceeded to calculate the exciton binding energies (E_b) of the reticular ratchets (Figures S65 and S66).[37,38] Our calculations reveal that D-CN-A with a larger band gap exhibits larger E_b values than its D-NC-A counterparts (Figure 3c), signifying a higher propensity for exciton formation in D-CN-A and an increased tendency for electron−hole separation in D-NC-A.[38,39] Furthermore, the differential charge density between the first excited state (S_1) and ground state (S_0) of the reticular ratchets demonstrated that the electrons and holes in Tpy-CN-Tt are less separated than those in Tpy-NC-Tt (Figure 3d), indicating a more facile exciton generation process in D-CN-A than that in D-NC-A (Figures S67−S77 and Table S5).[40] These calculation results align with the slower fluorescence decays (Figure S78 and Table S6), lower fluorescence quantum yields (Figure S79),[41] and stronger electron paramagnetic resonance signals observed in D-NC-A upon excitation (Figure S80).[42] In addition, ECL transients of Tpy-CN-Tt demonstrated more efficient exciton production compared with Tpy-NC-Tt, verifying a typical ratchet effect of directing the IRCT from the N-end to the C-end units for ECL emission (Figures 3e and S81−S91).

Reticular Ratchet Mechanism-Regulated ECL. To further investigate the ratchet effect of the reticular ratchets, femtosecond transient absorption spectroscopy was applied (Figure 4a−f). Tpy-CN-Tt and Tpy-NC-Tt exhibited ground state bleachings (GSBs) at 509 and 525 nm, respectively, which correspond to the absorbance of Tt units (Figures 4b,e and S35).[43,44] The separated charges were featured by excited state absorptions (ESAs) in Tpy-CN-Tt at 712 nm and Tpy-NC-Tt at 643 nm within 1.5 ps (Figure 4b).[45,46] Compared with Tpy-NC-Tt, the faster decay of both GSB and ESA for Tpy-CN-Tt signified more efficient electron−hole recombination (Figure 4c,f), which is in agreement with the larger E_b.[46,47] Therefore, the polar imine bond in Tpy-Tt functions as a ratchet tooth to accelerate exciton production for enhanced ECL.

Furthermore, we conducted 5000 fs NAMD simulations to evaluate the electron−hole combination process. By analyzing the energy and population of separated electrons and holes, we found that both the electrons and holes of Tpy-CN-Tt decay faster than those of Tpy-NC-Tt (Figure 4g), which is consistent with the above fs-TA results. NAMD simulations of Tpy-Ph and Tpa-Tz ratchets also exhibited a faster electron−hole combination of Tpa-CN-Tz and Tpy-CN-Ph (Figures S92−S94), verifying the efficient IRCT-directing abilities of the reticular ratchets.

We found that the D−A contrast caused band gap difference is proportional to ECL efficiency (reticular ratchet efficiency), and the faster charge transfer dynamics of D-CN-A COFs facilitated the ECL exciton generation in each pair of reticular ratchets (Figures S95−S97). An exponential correlation between the DFT-calculated dipole differences and the experimentally measured ECL efficiency ratio of each ratchet is established (Figure 4i):

$$\frac{\Phi_{ECL,CN}}{\Phi_{ECL,NC}} = e^{k\Delta Dipole_{imine}}$$

where $\Phi_{ECL,CN}/\Phi_{ECL,NC}$ and $\Delta Dipole_{imine}$ represent the ECL efficiency ratio and imine dipole difference in each reticular ratchet, respectively; and k is the corrected coefficient. Finally, a reticular ratchet-regulated ECL mechanism was proposed (Figure 4h). That is, steeper slopes are formed when electrons transfer from the C-end to N-end units, whereas gentler slopes arise when electrons transfer from the N-end to C-end units. The increase in the D−A contrast results in higher ratchet potentials due to electronic interactions between the D−A units and imine bonds. Consequently, higher D−A contrast leads to a more efficient IRCT in the D-CN-A system for luminous energy transduction from electric and chemical sources through the ratchet effect.

CONCLUSIONS

In summary, by employing the ratchet-directed ECL as a bridge between the charge transfer and ratchet effect, IRCT was delicately manipulated based on 10 pairs of D−A COFs with imine bonds of mutually reversed orientations. The polar imine bonds in the COFs acted as an efficient ratchet tooth for directing the electron transfer from N-end units toward C-end units, thereby yielding effective control over the ECL efficiency. The established correlation between ECL efficiency ratios and dipole differences highlights the prospect of designing efficient ECL emitters through the deliberate manipulation of the ratchet effect between D−A fragments. With the deepening of mechanism understanding, we anticipate that our research will drive progress in the fields of optoelectronics, photoelectrochemical devices, and beyond. This innovative concept of the reticular ratchet opens up new avenues for precise management of charge transfer within reticular materials, offering exciting opportunities in various scientific and technological domains.

ASSOCIATED CONTENT

Supporting Information

The Supporting Information is available free of charge at https://pubs.acs.org/doi/10.1021/jacs.4c03981.

Materials and methods, detailed synthesis, and additional characterization of the obtained COF pairs, ECL tests, and DFT calculations (PDF)

AUTHOR INFORMATION

Corresponding Authors

Shuai Yuan − *State Key Laboratory of Analytical Chemistry for Life Science, State Key Laboratory of Coordination*

https://doi.org/10.1021/jacs.4c03981
J. Am. Chem. Soc. 2024, 146, 16681−16688

Chemistry, Key Laboratory of Mesoscopic Chemistry of MOE, School of Chemistry and Chemical Engineering, Nanjing University, Nanjing 210023, China; orcid.org/0000-0003-3329-0481; Email: syuan@nju.edu.cn

Xiaojun Wu − *Key Laboratory of Precision and Intelligent Chemistry, School of Chemistry and Materials Sciences, and iChem, Hefei National Laboratory, University of Science and Technology of China, Hefei 230026, China;* orcid.org/0000-0003-3606-1211; Email: xjwu@ustc.edu.cn

Jianping Lei − *State Key Laboratory of Analytical Chemistry for Life Science, State Key Laboratory of Coordination Chemistry, Key Laboratory of Mesoscopic Chemistry of MOE, School of Chemistry and Chemical Engineering, Nanjing University, Nanjing 210023, China;* orcid.org/0000-0002-3594-180X; Email: jpl@nju.edu.cn

Authors

Rengan Luo − *State Key Laboratory of Analytical Chemistry for Life Science, State Key Laboratory of Coordination Chemistry, Key Laboratory of Mesoscopic Chemistry of MOE, School of Chemistry and Chemical Engineering, Nanjing University, Nanjing 210023, China*

Xiao Luo − *Key Laboratory of Precision and Intelligent Chemistry, School of Chemistry and Materials Sciences, and iChem, Hefei National Laboratory, University of Science and Technology of China, Hefei 230026, China*

Haocheng Xu − *State Key Laboratory of Analytical Chemistry for Life Science, State Key Laboratory of Coordination Chemistry, Key Laboratory of Mesoscopic Chemistry of MOE, School of Chemistry and Chemical Engineering, Nanjing University, Nanjing 210023, China*

Sushu Wan − *State Key Laboratory of Analytical Chemistry for Life Science, State Key Laboratory of Coordination Chemistry, Key Laboratory of Mesoscopic Chemistry of MOE, School of Chemistry and Chemical Engineering, Nanjing University, Nanjing 210023, China;* orcid.org/0000-0001-8666-9255

Haifeng Lv − *Key Laboratory of Precision and Intelligent Chemistry, School of Chemistry and Materials Sciences, and iChem, Hefei National Laboratory, University of Science and Technology of China, Hefei 230026, China;* orcid.org/0000-0001-9491-6367

Beier Zou − *State Key Laboratory of Analytical Chemistry for Life Science, State Key Laboratory of Coordination Chemistry, Key Laboratory of Mesoscopic Chemistry of MOE, School of Chemistry and Chemical Engineering, Nanjing University, Nanjing 210023, China*

Yufei Wang − *State Key Laboratory of Analytical Chemistry for Life Science, State Key Laboratory of Coordination Chemistry, Key Laboratory of Mesoscopic Chemistry of MOE, School of Chemistry and Chemical Engineering, Nanjing University, Nanjing 210023, China*

Tianrui Liu − *State Key Laboratory of Analytical Chemistry for Life Science, State Key Laboratory of Coordination Chemistry, Key Laboratory of Mesoscopic Chemistry of MOE, School of Chemistry and Chemical Engineering, Nanjing University, Nanjing 210023, China*

Chuang Wu − *State Key Laboratory of Analytical Chemistry for Life Science, State Key Laboratory of Coordination Chemistry, Key Laboratory of Mesoscopic Chemistry of MOE, School of Chemistry and Chemical Engineering, Nanjing University, Nanjing 210023, China*

Qizhou Chen − *State Key Laboratory of Analytical Chemistry for Life Science, State Key Laboratory of Coordination Chemistry, Key Laboratory of Mesoscopic Chemistry of MOE, School of Chemistry and Chemical Engineering, Nanjing University, Nanjing 210023, China*

Siqi Yu − *State Key Laboratory of Analytical Chemistry for Life Science, State Key Laboratory of Coordination Chemistry, Key Laboratory of Mesoscopic Chemistry of MOE, School of Chemistry and Chemical Engineering, Nanjing University, Nanjing 210023, China*

Pengfei Dong − *State Key Laboratory of Analytical Chemistry for Life Science, State Key Laboratory of Coordination Chemistry, Key Laboratory of Mesoscopic Chemistry of MOE, School of Chemistry and Chemical Engineering, Nanjing University, Nanjing 210023, China*

Yuxi Tian − *State Key Laboratory of Analytical Chemistry for Life Science, State Key Laboratory of Coordination Chemistry, Key Laboratory of Mesoscopic Chemistry of MOE, School of Chemistry and Chemical Engineering, Nanjing University, Nanjing 210023, China;* orcid.org/0000-0002-5910-1514

Kai Xi − *State Key Laboratory of Analytical Chemistry for Life Science, State Key Laboratory of Coordination Chemistry, Key Laboratory of Mesoscopic Chemistry of MOE, School of Chemistry and Chemical Engineering, Nanjing University, Nanjing 210023, China;* orcid.org/0000-0002-8770-5956

Huangxian Ju − *State Key Laboratory of Analytical Chemistry for Life Science, State Key Laboratory of Coordination Chemistry, Key Laboratory of Mesoscopic Chemistry of MOE, School of Chemistry and Chemical Engineering, Nanjing University, Nanjing 210023, China;* orcid.org/0000-0002-6741-5302

Complete contact information is available at: https://pubs.acs.org/10.1021/jacs.4c03981

Author Contributions

#R.L. and X.L. contributed equally to this work. The manuscript was written through contributions of all authors. All authors have given approval to the final version of the manuscript.

Notes

The authors declare no competing financial interest.

■ ACKNOWLEDGMENTS

This work was supported by the National Natural Science Foundation of China (22274071, 22234005, 22225301 22073087, and 22271141), the Natural Science Foundation of Jiangsu Province (BZ2021010 and BK20220765), the CAS Project for Young Scientists in Basic Research (YSBR-004), the Strategic Priority Research Program of the CAS (XDB0450101), the Fundamental Research Funds for the Central Universities (WK2060000038), Innovation Program for Quantum Science and Technology (2021ZD0303302), and the Super Computer Centre of USTCSCC and SCCAS.

■ REFERENCES

(1) Feynman, R. P.; Vernon, F. L. The Theory of a General Quantum System Interacting with a Linear Dissipative System. *Ann. Phys.* **1963**, *24*, 118−173.

(2) Ren, Y.; Jamagne, R.; Tetlow, D. J.; Leigh, D. A. A Tape-Reading Molecular Ratchet. *Nature* **2022**, *612*, 78−82.

(3) Simpson, G. J.; Persson, M.; Grill, L. Adsorbate Motors for Unidirectional Translation and Transport. *Nature* **2023**, *621*, 82−86.
(4) Hochberg, G. K. A.; Liu, Y.; Marklund, E. G.; Metzger, B. P. H.; Laganowsky, A.; Thornton, J. W. A Hydrophobic Ratchet Entrenches Molecular Complexes. *Nature* **2020**, *588*, 503−508.
(5) Schliwa, M.; Woehlke, G. Molecular Motors. *Nature* **2003**, *422*, 759−765.
(6) Erbas-Cakmak, S.; Leigh, D. A.; McTernan, C. T.; Nussbaumer, A. L. Artificial Molecular Machines. *Chem. Rev.* **2015**, *115*, 10081−10206.
(7) Yaghi, O. M.; Kalmutzki, M. J.; Diercks, C. S. *Introduction to Reticular Chemistry: Metal−Organic Frameworks and Covalent Organic Frameworks*. Wiley-VCH: Weinheim, Germany, 2019.
(8) Côté, A. P.; Benin, A. I.; Ockwig, N. W.; O'Keeffe, M.; Matzger, A. J.; Yaghi, O. M. Porous, Crystalline, Covalent Organic Frameworks. *Science* **2005**, *310*, 1166−1170.
(9) Uribe-Romo, F. J.; Hunt, J. R.; Furukawa, H.; Klock, C.; O'Keeffe, M.; Yaghi, O. M. A Crystalline Imine-Linked 3-D Porous Covalent Organic Framework. *J. Am. Chem. Soc.* **2009**, *131*, 4570−4571.
(10) Tan, K. T.; Ghosh, S.; Wang, Z.; Wen, F.; Rodríguez-San-Miguel, D.; Feng, J.; Huang, N.; Wang, W.; Zamora, F.; Feng, X.; Thomas, A.; Jiang, D. Covalent Organic Frameworks. *Nat. Rev. Methods Primers* **2023**, *3*, 1.
(11) Yaghi, O. M.; Li, G.; Li, H. Selective Binding and Removal of Guests in a Microporous Metal−Organic Framework. *Nature* **1995**, *378*, 703−706.
(12) Krause, S.; Feringa, B. L. Towards Artificial Molecular Factories from Framework-Embedded Molecular Machines. *Nat. Rev. Chem.* **2020**, *4*, 550−562.
(13) Feng, L.; Astumian, R. D.; Stoddart, J. F. Controlling Dynamics in Extended Molecular Frameworks. *Nat. Rev. Chem.* **2022**, *6*, 705−725.
(14) Feng, L.; Qiu, Y.; Guo, Q. H.; Chen, Z.; Seale, J. S. W.; He, K.; Wu, H.; Feng, Y.; Farha, O. K.; Astumian, R. D.; Stoddart, J. F. Active Mechanisorption Driven by Pumping Cassettes. *Science* **2021**, *374*, 1215−1221.
(15) Streater, D. H.; Kennehan, E. R.; Wang, D.; Fiankor, C.; Chen, L.; Yang, C.; Li, B.; Liu, D.; Ibrahim, F.; Hermans, I.; Kohlstedt, K. L.; Luo, L.; Zhang, J.; Huang, J. Control over Charge Separation by Imine Structural Isomerization in Covalent Organic Frameworks with Implications on CO_2 Photoreduction. *J. Am. Chem. Soc.* **2024**, *146*, 4489−4499.
(16) Bard, A. J. *Electrogenerated Chemiluminescence*. Marcel Dekker: New York, 2004.
(17) Ding, Z. F.; Quinn, B. M.; Haram, S. K.; Pell, L. E.; Korgel, B. A.; Bard, A. J. Electrochemistry and Electrogenerated Chemiluminescence from Silicon Nanocrystal Quantum Dots. *Science* **2002**, *296*, 1293−1296.
(18) Luo, R.; Zhu, D.; Ju, H.; Lei, J. Reticular Electrochemiluminescence Nanoemitters: Structural Design and Enhancement Mechanism. *Acc. Chem. Res.* **2023**, *56*, 1920−1930.
(19) Luo, R.; Lv, H.; Liao, Q.; Wang, N.; Yang, J.; Li, Y.; Xi, K.; Wu, X.; Ju, H.; Lei, J. Intrareticular Charge Transfer Regulated Electrochemiluminescence of Donor-Acceptor Covalent Organic Frameworks. *Nat. Commun.* **2021**, *12*, 6808.
(20) Zhu, D.; Zhang, Y.; Bao, S.; Wang, N.; Yu, S.; Luo, R.; Ma, J.; Ju, H.; Lei, J. Dual Intrareticular Oxidation of Mixed-Ligand Metal-Organic Frameworks for Stepwise Electrochemiluminescence. *J. Am. Chem. Soc.* **2021**, *143*, 3049−3053.
(21) Li, Y. J.; Cui, W. R.; Jiang, Q. Q.; Wu, Q.; Liang, R. P.; Luo, Q. X.; Qiu, J. D. A General Design Approach toward Covalent Organic Frameworks for Highly Efficient Electrochemiluminescence. *Nat. Commun.* **2021**, *12*, 4735.
(22) Kuhnke, K.; Große, C.; Merino, P.; Kern, K. Atomic-Scale Imaging and Spectroscopy of Electroluminescence at Molecular Interfaces. *Chem. Rev.* **2017**, *117*, 5174−5222.
(23) Roeffaers, M. B.; Sels, B. F.; Uji, I. H.; De Schryver, F. C.; Jacobs, P. A.; De Vos, D. E.; Hofkens, J. Spatially Resolved Observation of Crystal-Face-Dependent Catalysis by Single Turnover Counting. *Nature* **2006**, *439*, 572−575.
(24) Zhang, J.; Arbault, S.; Sojic, N.; Jiang, D. Electrochemiluminescence Imaging for Bioanalysis. *Annu. Rev. Anal. Chem.* **2019**, *12*, 275−295.
(25) Dong, J.; Lu, Y.; Xu, Y.; Chen, F.; Yang, J.; Chen, Y.; Feng, J. Direct Imaging of Single-Molecule Electrochemical Reactions in Solution. *Nature* **2021**, *596*, 244−249.
(26) Paul, K. K.; Kim, J.-H.; Lee, Y. H. Hot Carrier Photovoltaics in van der Waals Heterostructures. *Nat. Rev. Phys.* **2021**, *3*, 178−192.
(27) Tran, L. D.; Presley, K. F.; Streit, J. K.; Carpena-Núñez, J.; Beagle, L. K.; Grusenmeyer, T. A.; Dalton, M. J.; Vaia, R. A.; Drummy, L. F.; Glavin, N. R.; Baldwin, L. A. Divergent Properties in Structural Isomers of Triphenylamine-Based Covalent Organic Frameworks. *Chem. Mater.* **2022**, *34*, 529−536.
(28) Yang, J.; Ghosh, S.; Roeser, J.; Acharjya, A.; Penschke, C.; Tsutsui, Y.; Rabeah, J.; Wang, T.; Djoko Tameu, S. Y.; Ye, M. Y.; Gruneberg, J.; Li, S.; Li, C.; Schomacker, R.; Van De Krol, R.; Seki, S.; Saalfrank, P.; Thomas, A. Constitutional Isomerism of the Linkages in Donor-Acceptor Covalent Organic Frameworks and Its Impact on Photocatalysis. *Nat. Commun.* **2022**, *13*, 6317.
(29) Dong, W.; Qin, Z.; Wang, K.; Xiao, Y.; Liu, X.; Ren, S.; Li, L. Isomeric Oligo(Phenylenevinylene)-Based Covalent Organic Frameworks with Different Orientation of Imine Bonds and Distinct Photocatalytic Activities. *Angew. Chem., Int. Ed.* **2023**, *62*, No. e202216073.
(30) Li, X.; Yu, J.; Jaroniec, M.; Chen, X. Cocatalysts for Selective Photoreduction of CO_2 into Solar Fuels. *Chem. Rev.* **2019**, *119*, 3962−4179.
(31) Joshi, T.; Chen, C.; Li, H.; Diercks, C. S.; Wang, G.; Waller, P. J.; Li, H.; Bredas, J. L.; Yaghi, O. M.; Crommie, M. F. Local Electronic Structure of Molecular Heterojunctions in a Single-Layer 2D Covalent Organic Framework. *Adv. Mater.* **2019**, *31*, No. e1805941.
(32) Yue, J.-Y.; Song, L.-P.; Pan, Z.-X.; Yang, P.; Ma, Y.; Xu, Q.; Tang, B. Regulating the H_2O_2 Photosynthetic Activity of Covalent Organic Frameworks through Linkage Orientation. *ACS Catal.* **2024**, *14*, 4728−4737.
(33) Bao, B.; Li, R.; Hao, Y.; Xiao, R.; Hou, C.; Li, Y.; Zhang, Q.; Li, K.; Wang, H. Tuning Electron Transfer in Pyrene-Based Two Dimensional Covalent Organic Frameworks: Unveiling the Impact of Semi-isomerism on Physicochemical Properties. *Chem. Mater.* **2024**, *36*, 2880−2887.
(34) Qian, Y.; Han, Y.; Zhang, X.; Yang, G.; Zhang, G.; Jiang, H. L. Computation-Based Regulation of Excitonic Effects in Donor-Acceptor Covalent Organic Frameworks for Enhanced Photocatalysis. *Nat. Commun.* **2023**, *14*, 3083.
(35) Pulay, P.; Fogarasi, G.; Pang, F.; Boggs, J. E. Systematic *Ab Initio* Gradient Calculation of Molecular Geometries, Force Constants, and Dipole Moment Derivatives. *J. Am. Chem. Soc.* **1979**, *101*, 2550−2560.
(36) Cheetham, A. K.; Dobson, C. M.; Grey, C. P.; Jakeman, R. J. B. Paramagnetic Shift Probes in High-Resolution Solid-State NMR. *Nature* **1987**, *328*, 706−707.
(37) Deng, Y.; Lin, X.; Fang, W.; Di, D.; Wang, L.; Friend, R. H.; Peng, X.; Jin, Y. Deciphering Exciton-Generation Processes in Quantum-Dot Electroluminescence. *Nat. Commun.* **2020**, *11*, 2309.
(38) Yu, H.; Wang, D. Suppressing the Excitonic Effect in Covalent Organic Frameworks for Metal-Free Hydrogen Generation. *JACS Au* **2022**, *2*, 1848−1856.
(39) Choi, J. H.; Cui, P.; Lan, H.; Zhang, Z. Linear Scaling of the Exciton Binding Energy versus the Band Gap of Two-Dimensional Materials. *Phys. Rev. Lett.* **2015**, *115*, No. 066403.
(40) Gillett, A. J.; Privitera, A.; Dilmurat, R.; Karki, A.; Qian, D.; Pershin, A.; Londi, G.; Myers, W. K.; Lee, J.; Yuan, J.; Ko, S. J.; Riede, M. K.; Gao, F.; Bazan, G. C.; Rao, A.; Nguyen, T. Q.; Beljonne, D.; Friend, R. H. The Role of Charge Recombination to Triplet Excitons in Organic Solar Cells. *Nature* **2021**, *597*, 666−671.
(41) Passarelli, J. V.; Mauck, C. M.; Winslow, S. W.; Perkinson, C. F.; Bard, J. C.; Sai, H.; Williams, K. W.; Narayanan, A.; Fairfield, D. J.;

Hendricks, M. P.; Tisdale, W. A.; Stupp, S. I. Tunable Exciton Binding Energy in 2D Hybrid Layered Perovskites through Donor-Acceptor Interactions within the Organic Layer. *Nat. Chem.* **2020**, *12*, 672−682.
(42) Qin, C.; Wu, X.; Tang, L.; Chen, X.; Li, M.; Mou, Y.; Su, B.; Wang, S.; Feng, C.; Liu, J.; Yuan, X.; Zhao, Y.; Wang, H. Dual Donor-Acceptor Covalent Organic Frameworks for Hydrogen Peroxide Photosynthesis. *Nat. Commun.* **2023**, *14*, 5238.
(43) Jakowetz, A. C.; Hinrichsen, T. F.; Ascherl, L.; Sick, T.; Calik, M.; Auras, F.; Medina, D. D.; Friend, R. H.; Rao, A.; Bein, T. Excited-State Dynamics in Fully Conjugated 2D Covalent Organic Frameworks. *J. Am. Chem. Soc.* **2019**, *141*, 11565−11571.
(44) Zhang, X.; Geng, K.; Jiang, D.; Scholes, G. D. Exciton Diffusion and Annihilation in an sp^2 Carbon-Conjugated Covalent Organic Framework. *J. Am. Chem. Soc.* **2022**, *144*, 16423−16432.
(45) Kim, T. W.; Jun, S.; Ha, Y.; Yadav, R. K.; Kumar, A.; Yoo, C.-Y.; Oh, I.; Lim, H.-K.; Shin, J. W.; Ryoo, R.; Kim, H.; Kim, J.; Baeg, J.-O.; Ihee, H. Ultrafast Charge Transfer Coupled with Lattice Phonons in Two-Dimensional Covalent Organic Frameworks. *Nat. Commun.* **2019**, *10*, 1873.
(46) Pan, Q.; Abdellah, M.; Cao, Y.; Lin, W.; Liu, Y.; Meng, J.; Zhou, Q.; Zhao, Q.; Yan, X.; Li, Z.; Cui, H.; Cao, H.; Fang, W.; Tanner, D. A.; Abdel-Hafiez, M.; Zhou, Y.; Pullerits, T.; Canton, S. E.; Xu, H.; Zheng, K. Ultrafast Charge Transfer Dynamics in 2D Covalent Organic Frameworks/Re-Complex Hybrid Photocatalyst. *Nat. Commun.* **2022**, *13*, 845.
(47) Yang, S.; Streater, D.; Fiankor, C.; Zhang, J.; Huang, J. Conjugation- and Aggregation-Directed Design of Covalent Organic Frameworks as White-Light-Emitting Diodes. *J. Am. Chem. Soc.* **2021**, *143*, 1061−1068.

https://doi.org/10.1021/jacs.4c03981
J. Am. Chem. Soc. 2024, 146, 16681−16688